Stability Criteria for Nanocrystalline Alloys

Arvind R. Kalidindi[1] and Christopher A. Schuh[1*]

[1] Department of Materials Science and Engineering, Massachusetts Institute of Technology, 77 Massachusetts Avenue, Cambridge, MA, 02139, USA.

* corresponding author: Tel.: +1 617-253-6901; email: schuh@mit.edu

Abstract

Alloying nanocrystalline materials to stabilize them against grain growth is proving a critical enabling strategy for the processing and usage of bulk nanocrystalline parts. Alloying elements that segregate strongly to grain boundaries can lead to a preference for nanocrystalline structure, and to be most stable the grain boundary segregated state would need to be preferred to forming any other phase or solute configuration, including a solid solution, ordered compounds, or solute precipitates. In this paper, a stability criterion is developed by comparing the enthalpy of the grain boundary segregated state against such stable bulk phases. This enthalpic criterion is also translated into a lattice model framework to enable the use of Monte Carlo simulations to incorporate entropic and geometric effects in assessing nanocrystalline stability. Monte Carlo simulations show that entropy can play a role in stabilizing nanocrystalline states, leading to duplex structures, and also in forming a grain boundary network preferentially over a disordered or amorphous-like bulk phase.

Keywords: nanocrystalline, alloy, grain boundary, segregation, intermetallic

1. Introduction

Achieving grain sizes on the nanometer length scale (< 100 nm) leads to unique property combinations, both structural [1-5] and functional [6-8], due to the dominant presence of grain boundaries. This refinement is however accompanied by a large driving force for grain growth: doubling the grain size of a nanocrystalline material leads to a ~1000 times larger decrease in grain boundary area than does doubling a micron-scale grain size. This can cause rapid grain growth at relatively low homologous temperatures in nanocrystalline materials [9-12], which makes it difficult to produce bulk nanocrystalline parts and challenges their use in service.

One way to suppress this structural instability is to alter the energy landscape of the material through chemistry. Alloying can play two roles in shaping the energy landscape to increase resistance to grain growth: the alloying element can increase the energetic barrier (or activation energy) to grain growth through solute drag and/or Zener pinning, or it can decrease the energetic benefit of grain growth through grain boundary segregation according to the Gibbs adsorption isotherm [13-15]. In the latter case, Weissmüller showed that the driving force for grain growth can be eliminated if the energetic preference of grain boundary sites for the solute is strong enough, as governed by the enthalpy of grain boundary segregation, ΔH_{seg} [13]. This route to stabilizing nanocrystalline materials has been gaining favor [1, 16-33] as it can not only produce a more reliable form of stability but is also potentially easier to design for; due to its thermodynamic nature, achieving this stability mostly depends on choosing the right alloy combination.

The first alloy selection criterion to stabilize the nanocrystalline state was proposed by Weissmüller, based on the Gibbs adsorption isotherm [13]:

$$\Delta H_{\mathrm{seg}} > \frac{\gamma}{\Gamma} - \mathrm{k_B} T \ln(X) \quad (1)$$

The inequality states that the enthalpy of grain boundary segregation, ΔH_{seg}, must be large enough to overcome the enthalpic penalty of the grain boundary, γ/Γ (γ: pure solvent grain boundary energy; Γ: solute excess in the grain boundary), and the entropic advantage of a crystalline solid solution ($\mathrm{k_B}$: Boltzmann's constant; T: temperature; X: intragranular solute concentration). While this equation only applies in the dilute limit, it has been extended using regular solution models, which produce more general forms of Eq. 1 [22-27]. When these criteria have been used to select stable alloy chemistries, the resulting nanocrystalline states are usually found to be stable at low homologous temperatures. However, when the temperature is increased, second phases often form at grain boundaries where the solute is enriched, as seen in Ni-P, Co-P, Fe-Zr and Ni-W [28-33]. Such precipitation is accompanied by subsequent grain growth when the grain boundaries are no longer sufficiently stabilized by solutes, which are instead precipitated in the second phase. Thus, stability against grain growth in such alloys is actually a form of metastability, and a deeper level of stability would be a nanocrystalline state in which grain boundary segregation is preferred over the formation of bulk phases.

A systematic way to study the stability of the grain boundary segregated state with respect to bulk solute-containing phases is to include the grain boundary segregated state on a bulk free energy diagram. Using regular solution models to describe the free energy of the segregated grain boundary as a function of global solute concentration, Murdoch and Schuh [23] developed criteria for stability of a grain boundary segregated state against both grain growth and second phase formation for positive enthalpy of mixing (ΔH_{mix}) systems using the form:

$$\Delta H_{\text{seg}} > c(\Delta H_{\text{mix}})^{a} \quad (2)$$

where the coefficients *a* and *c* depend on the homologous temperature and were fitted to the results of the regular solution model. For a given temperature, two sets of *a* and *c* describe stability: one specifies the criterion for metastability, where formation of a solute-rich phase is not considered, and the other, which has a larger *c* and therefore also a larger threshold value for ΔH_{seg}, specifies stability both against grain growth and phase separation. This same approach can be used to study stability against compound formation, as was done for Fe-Zr alloys by Zhou and Luo [24], but a general stability criterion for a grain boundary segregated state against compound formation has not yet been developed.

The reliability of the stability criterion in Eq. 2 is limited by the regular solution assumption, which assumes a random distribution of solute atoms along the grain boundary. This is a poor assumption; grain boundary segregation occurs largely because of the diversity of possible solute sites in a boundary, and solute is expected to populate such sites in increasing order of energetic relief. Solute ordering is not only expected, but routinely observed in grain boundary segregation [34-40]. In order to relieve regular solution assumptions, Chookajorn and Schuh developed a lattice-based Monte Carlo approach that considers both bulk and nanocrystalline configurations within its phase space and determines the free-energy minimizing microstructure [41]. Because this simulation no longer constrains the possible equilibrium states to either be a bulk state or a segregated nanocrystalline state, it is a powerful tool for studying the equilibria of strongly grain boundary segregating alloys. One such observation was the existence of a duplex nanostructure wherein solute-rich precipitates form alongside solute segregated grain boundaries, which is difficult to consider analytically [41, 42]. They also used their model to develop stability criteria:

$$\text{Metastability:} \quad \Delta H_{\text{seg}} > \frac{1}{2}\Delta H_{\text{mix}} + k\gamma \tag{3}$$

$$\text{Stability:} \quad \Delta H_{\text{seg}} > \Delta H_{\text{mix}} + k\gamma \tag{4}$$

where γ is the grain boundary energy of the pure solvent and k is a scaling factor used to estimate the grain boundary area per atom (approximated in that work as the atomic volume of solvent divided by the grain boundary thickness [22]). This stability criterion conforms to physical intuition about the energy relationship necessary for stability in a positive enthalpy of mixing system: in order for the grain boundary segregated state to be the lowest energy configuration, it must reduce the energy enough to offset both the energy penalty of forming a grain boundary ($k\gamma$) and the energy benefit of forming a solute-rich precipitate (ΔH_{mix}). Note that these criteria consider enthalpic preference only, because the Monte Carlo method was used to handle configurational entropy. To complete the analogy of these expressions with Eq. (1) would require the addition of an entropy term (e.g. $\mathrm{k_B}T\ln(X)$).

The criteria in Eqs. 3 and 4 were developed only for alloys with positive enthalpies of mixing, and further tacitly assuming that the enthalpy of the grain boundary segregated state is well-represented by the solute-solvent atom interaction energy at a grain boundary. While these criteria present an interesting advance, the number of alloy systems with a positive enthalpy of mixing is small: considering transition metal pairs, roughly 40% have a positive enthalpy of mixing whereas 60% have a negative one and/or form intermetallic compounds [43]. Furthermore, the most widely studied and/or commercially successful grain-boundary segregating systems are compound formers (i.e., Ni-W, Ni-P, Co-P, Fe-Zr as described above). There is therefore a need to extend the stability criteria above to non-regular systems with negative enthalpies of mixing, and our purpose in this paper is to do so. By more rigorously considering the ordered configuration

of solute at the grain boundaries and the effect of ordered compounds, we first develop an analytical criterion and subsequently cast it into lattice model terms in order to inform Monte Carlo explorations of nanocrystalline stability.

2. Stability Criterion from Enthalpic Considerations

Grain boundary segregation, like precipitation, is largely believed to be an enthalpic effect, and is thus a form of chemical ordering. The competition between different ordered states can be resolved by determining which ordered state provides the lowest enthalpy for the alloy system, as is typically done for ordered compounds in developing 0 K phase diagrams [43-45]. The energies of ordered states as a function of composition can be compared on an energy diagram such as Fig. 1 to determine regimes of stability, where here we particularly focus on solute-lean compositions without loss of generality. The enthalpy of the binary alloy system with an ordered phase, H_{ord}, can generally be written as:

$$H_{\mathrm{ord}} = \left(1 - \frac{X}{x_{\mathrm{s}}^{\mathrm{C}}}\right) E_{\mathrm{A}} + \frac{X}{x_{\mathrm{s}}^{\mathrm{C}}} E_{\mathrm{C}} \tag{5}$$

where E_{A} and E_{C} are the enthalpy per atom of the pure solvent and ordered compound, respectively, X is the global solute concentration, and $x_{\mathrm{s}}^{\mathrm{C}}$ is the stoichiometry of the compound (i.e. the fraction of atoms in the compound that are solute atoms). This expression defines the common tangent line of an ordered phase and the pure solvent phase, and is also applicable to positive enthalpy of mixing systems by setting $E_{\mathrm{C}} = E_{\mathrm{B}}$ and $x_{\mathrm{s}}^{\mathrm{C}} = 1$, where E_{B} is the enthalpy per atom of a pure solute phase.

Generally, a grain boundary segregated state at thermodynamic equilibrium is a complexion [34], i.e., a defined equilibrium atomic configuration at the interface separating grains. For the developments that follow, we find it useful to adopt the view that this complexion is more specifically a 2D compound [35, 36] as it will exhibit a chemically ordered configuration that, similar to a 3D ordered phase, can be described using an effective enthalpy per atom, E_{GB}, and a stoichiometry, $x_{\mathrm{s}}^{\mathrm{GB}}$, which is the fraction of atoms in the grain boundary compound that are solute. Therefore, the enthalpy of a nanocrystalline alloy, H_{GB}, with a solute-enriched grain boundary can also be written in the same format as Eq. 5:

$$H_{\mathrm{GB}} = \left(1 - \frac{X}{x_{\mathrm{s}}^{\mathrm{GB}}}\right) E_{\mathrm{A}} + \frac{X}{x_{\mathrm{s}}^{\mathrm{GB}}} E_{\mathrm{GB}} \tag{6}$$

Under this representation, the enthalpy of the nanocrystalline alloy follows a common tangent line as shown in Fig. 1, between the pure solvent phase and the grain boundary compound. The implication of this common tangent line is that at compositions below the stoichiometry of the grain boundary compound, the volume fraction of the grain boundary compound decreases proportionally according to a lever rule. In a system with fixed grain boundary area, one might envision patches of grain boundary with the equilibrium grain boundary compound that grow in area as the global concentration is increased. In the more general case where grain boundary area is unconstrained and can equilibrate, one expects the area density of grain boundaries to increase with composition and the entire grain boundary to be at the grain boundary compound stoichiometry. This representation is consistent with the behavior of regular solution models of nanocrystalline stability [23, 24]. At the stoichiometric composition, this approach predicts a system fully composed of the grain boundary segregated state/compound, which is not a well-defined condition. For example, in prior work the grain boundary segregated state has been likened

to an amorphous configuration near stoichiometry [23, 24, 41]. In the present work we will consider systems with solute concentrations well below the grain boundary compound stoichiometry; the grain boundary compound thus forms in a lever-rule fashion with the terminal solvent phase.

Finally, we must consider whether forming a grain boundary segregated state is preferred with respect to forming a bulk ordered phase. This would occur using the above definitions when $H_{\mathrm{GB}} < H_{\mathrm{ord}}$. The stability criterion for forming a nanocrystalline state is thus:

$$\frac{1}{x_s^{\mathrm{GB}}}(E_{\mathrm{GB}} - E_{\mathrm{A}}) < \frac{1}{x_s^{\mathrm{C}}}(E_{\mathrm{C}} - E_{\mathrm{A}}) \tag{7}$$

To translate this into alloy design terms, the per-atom enthalpies of the ordered states ($E_{\mathrm{GB}}, E_{\mathrm{C}}$) should be replaced by expressions for the global enthalpies of compound formation, ΔH_{form}, and grain boundary segregation, ΔH_{seg}. For the compound, this relationship is:

$$\Delta H_{\mathrm{form}} = E_{\mathrm{C}} - (1 - x_s^{\mathrm{C}})E_{\mathrm{A}} - x_s^{\mathrm{C}} E_{\mathrm{B}} \tag{8}$$

An enthalpy of formation can also be defined for the grain boundary segregated state, however it is better to define the grain boundary compound energy as a function of ΔH_{seg} as this is the more traditional thermodynamic parameter, defined as the change in enthalpy of the system upon swapping a solute atom at the grain boundary with a solvent atom in the grain, and defined such that grain boundary segregation is expected when $\Delta H_{\mathrm{seg}} > 0$. Substituting a solute atom at the grain boundary for a solvent atom replaces one unit of the grain boundary compound with a region of pure solvent grain boundary. This results in an enthalpy change of $\frac{1}{x_s^{\mathrm{GB}}}\left(E_{\mathrm{GB}}^{\mathrm{A}} - E_{\mathrm{GB}}\right)$, where $E_{\mathrm{GB}}^{\mathrm{A}}$ is the enthalpy per atom of a pure solvent grain boundary. In the crystalline region, removing a solvent atom from a pure solvent matrix requires an energy of $2E_{\mathrm{A}}$ and after substitution of a

solute atom, the energy of the site, $E_{\mathrm{B\ in\ A}}$, can be written in terms of the enthalpy of mixing: $\Delta H_{\mathrm{mix}} = E_{\mathrm{B\ in\ A}} - E_{\mathrm{B}} - E_{\mathrm{A}}$. As a result, a general expression for the enthalpy of grain boundary segregation is:

$$\Delta H_{\mathrm{seg}} = \Delta H_{\mathrm{mix}} + E_B - E_A - \frac{1}{x_{\mathrm{s}}^{\mathrm{GB}}}\left(E_{\mathrm{GB}} - E_{\mathrm{GB}}^{\mathrm{A}}\right) \tag{9}$$

Using the relationships in Eqs. 8 and 9, the criterion in Eq. 7 for the stability of a grain boundary segregated state with respect to forming second phases can be written as:

$$\Delta H_{\mathrm{seg}} > \Delta H_{\mathrm{mix}} - \frac{1}{x_{\mathrm{s}}^{\mathrm{c}}}\Delta H_{\mathrm{form}} + k\gamma \tag{10}$$

where $k\gamma$ is the excess energy of a pure A grain boundary, $\frac{1}{x_{\mathrm{s}}^{\mathrm{GB}}}\left(E_{\mathrm{GB}}^{\mathrm{A}} - E_{\mathrm{A}}\right)$, where just as in Eqs. 3 and 4, *k* converts the grain boundary energy from energy/area to energy/atom.

The criterion of Eq. 10 satisfies basic intuition for stabilizing grain boundaries with solute: a larger enthalpy of grain boundary segregation is required if the excess grain boundary energy that must be overcome is larger and if the crystal can undergo a larger drop in enthalpy by compound formation $\left(\Delta H_{\mathrm{mix}} - \frac{1}{x_{\mathrm{s}}^{\mathrm{c}}}\Delta H_{\mathrm{form}}\right)$. If this criterion is met, the energy of the system has a minimum at a particular grain size that depends on the solute concentration as seen by Chookajorn and Schuh [41]; decreasing the grain size from equilibrium results in an energetic penalty for forming pure solvent grain boundary and increasing the grain size results in an increase in energy for forming the bulk ordered phase instead of the grain boundary compound. For stability against phase separation into a solute precipitate in positive enthalpy of mixing systems, this same criterion holds with $\Delta H_{\mathrm{form}} = 0$. Alternatively, a grain boundary segregated state can be stable with respect

to grain growth alone, but only metastable with respect to forming a second phase. The metastability criterion thus does not include the enthalpy associated with second-phase formation:

$$\Delta H_{\text{seg}} > k\gamma \tag{11}$$

The metastability criterion attained in this manner is essentially the same as the one proposed by Weissmüller (Eq. 1), though Eq. 11 does not consider the entropy associated with forming a solid solution and thus is expected to underestimate the threshold for metastability.

The criteria for nanocrystalline stability established in Eqs. 10 and 11 are conveniently written in terms of bulk thermodynamic parameters that can be estimated for most binary alloy systems and guide the selection of alloying elements for nanocrystalline materials. The enthalpies of grain boundary segregation and solid-state mixing can be estimated empirically using a Miedema approach [48, 49]. The enthalpies of formation of binary compounds can be calculated by density functional theory and are readily attainable from the Open Quantum Materials Database [43]. While many compounds are often stable in the same binary system at different compositions, we suggest using the compound that is stable at the lowest stoichiometry as alloying for nanocrystalline stability is typically done at low compositions and this is the regime for which Eqs.10 and 11 apply. For the enthalpic penalty of the grain boundary, $k\gamma$, the pure element grain boundary energy can be estimated as one-third of the surface energy calculated from a Miedema model [49]. The coefficient, *k*, when applied in Section 6, will be approximated as the molar volume [50] divided by the grain boundary thickness (estimated as 5 Å). This approximation of *k*, which was also used in previous work [16,19,22,23,41] to convert the units of grain boundary energy to energy per mole, could be treated more completely, for example by more directly incorporating the packing density of atomic planes and the excess volume of the grain boundary.

3. Design Map for Stable Nanocrystalline Alloys

The criteria from Eqs. 10 and 11 delineate a stability map as shown in Fig. 2a, which classifies the stability of the grain boundary segregated state as a function of bulk thermodynamic parameters. On this stability map, one axis measures the enthalpy gained by forming a grain boundary segregated state (ΔH_{seg}) and the other measures the enthalpy gained by forming a crystalline second phase ($\Delta H_{\mathrm{mix}} - \frac{1}{x_{\mathrm{s}}^{\mathrm{c}}} \Delta H_{\mathrm{form}}$).

The existence of alloying combinations that meet the stability criterion thus requires that some alloys possess an enthalpy of grain boundary segregation that is sufficiently larger than the enthalpy gained by forming a second phase. This may seem unlikely due to the experimentally-observed relationship between the terminal solubility of a crystalline second phase and the enrichment factor (measure of excess solute) at the grain boundary [38,51], which is often interpreted as meaning that the enthalpies of grain boundary segregation and second phase formation are highly correlated, or $\Delta H_{\mathrm{seg}} \approx (\Delta H_{\mathrm{mix}} - \frac{1}{x_{\mathrm{s}}^{\mathrm{c}}} \Delta H_{\mathrm{form}})$ in the terms of our criterion.

To test whether this correlation is too strong for the stability criterion to be satisfied in physically realizable alloys, we determined ΔH_{seg}, ΔH_{mix}, and $\frac{1}{x_{\mathrm{s}}^{\mathrm{c}}} \Delta H_{\mathrm{form}}$ values (as described in the previous section) for a large number of transition metal – transition metal binary alloy pairs and plotted them on the same axes as the stability map (Figure 2b). Indeed, a positive correlation between the second phase and grain boundary segregation energies seems to exist as the points largely follow the trend of the solid line. However, there is a substantial amount of spread; the

dashed line represents the stability criterion when $k\gamma$ is 20 kJ/mol and it is observed that a number of alloy pairs satisfy the criterion for a stable nanocrystalline state.

The relatively large data spread in Figure 2b is not entirely surprising. The experimentally-observed correlation between terminal solubility and enrichment factor at the grain boundary has a spread of roughly one order of magnitude in the enrichment factor [38,51]. Furthermore, different ordered configurations in crystalline phases of the same alloy often vary in energy by dozens of kJ/mol, and thus it is reasonable to expect ordered 2D compounds to differ in energy from 3D compounds by energies on that order of magnitude as well.

4. Lattice Model Representation

Our stability and metastability criteria as developed in Section 2 are enthalpic and do not consider the entropy of the different ordered states or the presence of interphase boundaries. We favor the inclusion of configurational entropy effects using a lattice-based model, as it is a classical method for accounting for such effects and also opens the door to Monte Carlo exploration of the preferred structural configurations as a function of temperature and composition.

Equilibrium states of a bulk, single crystalline alloy in a lattice model (an Ising model for binary alloys) are determined by identifying the configuration of chemical species that minimizes the free energy of the alloy system. To incorporate the possible presence of grain boundaries, each lattice site carries two pieces of information: 1) the chemical identity of the species, and 2) a grain number denoting the grain allegiance of the atom at that site. Crystalline bonds are defined between neighboring atoms with the same grain number, and alternatively grain boundary bonds exist if the atoms have different grain numbers. The phase space of this model is thus any chemical

configuration on the lattice sites, with any set of bonds between lattice sites being grain boundary bonds. The equilibrium configuration can be determined using a Monte Carlo algorithm [41,46].

The equilibrium configuration is based on the defined interatomic potential. For positive enthalpy of mixing systems a nearest neighbor, pairwise potential with six bond energies was sufficient to provide distinct energies for grain boundary segregated states, solute precipitates, and solid solution phases, which could then be sampled by Monte Carlo to select the lowest free energy configuration [41]. These six pairwise bond energies are $\{E^{\mathrm{c}}_{\mathrm{AA}}, E^{\mathrm{c}}_{\mathrm{AB}}, E^{\mathrm{c}}_{\mathrm{BB}}, E^{\mathrm{gb}}_{\mathrm{AA}}, E^{\mathrm{gb}}_{\mathrm{AB}}, E^{\mathrm{gb}}_{\mathrm{BB}}\}$ where the subscript specifies the chemical identity of the two atoms bonded – solvent (A) and solute (B) – and the superscript denotes the nature of the bond – crystalline (c) and grain boundary (gb). However, the pairwise potential does not correctly produce bulk ordered phases in a lattice model, and multi-body terms are generally required. A complicated interatomic potential can be avoided by using the compound unit approach, which can incorporate compounds with known structure and formation energy into a lattice model [47]. This introduces an additional energy, which can conveniently be represented as an effective pairwise bond energy, $E^{\mathrm{c}}_{\mathrm{A_xB}}$.

At low temperatures, grain boundary segregation occurs in the lattice model when the lowest enthalpy compound at the grain boundary has a stoichiometry that is higher than the global solute concentration. Fig. 3a shows the grain boundary compound observed by Chookajorn and Schuh in a body-centered cubic (BCC) lattice when $E^{\mathrm{gb}}_{\mathrm{AB}}$ is lower than the mean of $E^{\mathrm{gb}}_{\mathrm{AA}}$ and $E^{\mathrm{gb}}_{\mathrm{BB}}$. The enthalpy of grain boundary segregation can be determined for a set of bond energies by measuring the change in enthalpy of a bicrystal from a random distribution of solute atoms to the equilibrium configuration and dividing by the change in the number of solutes residing at the grain boundary [41]. In order to relate the lattice model to physical systems, however, the inverse relationship needs to be determined: a known enthalpy of grain boundary segregation for an alloy

system must be described in terms of appropriate bond energies in the lattice model such that the enthalpy of segregation is achieved accurately in the simulation. Here, we estimate this relationship for this particular grain boundary compound by calculating the change in energy from swapping a solute atom in the crystal with a solvent atom in the grain boundary (z is the coordination number):

$$\Delta H_{\text{seg}} = \frac{z}{2}(E^{\text{c}}_{\text{AB}} - E^{\text{c}}_{\text{AA}} + E^{\text{gb}}_{\text{AA}} - E^{\text{gb}}_{\text{AB}}) \tag{12}$$

This relationship can equivalently be produced from Eq. 9 by using standard relationships ($\Delta H_{\text{mix}} = z\left(E^{\text{c}}_{\text{AB}} - \frac{E^{\text{c}}_{\text{AA}}+E^{\text{c}}_{\text{BB}}}{2}\right)$, $E_{\text{A}} = \frac{z}{2}E^{\text{c}}_{\text{AA}}$, $E_{\text{B}} = \frac{z}{2}E^{\text{c}}_{\text{BB}}$) and average grain boundary compound energies, which in this case are: $E^{\text{A}}_{\text{GB}} = \frac{z}{6}\left(E^{\text{gb}}_{\text{AA}} + 2E^{\text{c}}_{\text{AA}}\right)$ and $E_{\text{GB}} = \frac{z}{6}\left(E^{\text{gb}}_{\text{AB}} + E^{\text{c}}_{\text{AA}} + E^{\text{c}}_{\text{AB}}\right)$, where three layers of atoms are necessary to define the grain boundary compound ($x^{\text{GB}}_{\text{s}} = 1/3$).

The efficacy of Eq. 12 is evaluated by comparing the enthalpy of grain boundary segregation as calculated by this equation with the enthalpy of grain boundary segregation measured through a fixed bicrystal Monte Carlo simulation with the same pairwise bond energies. Fig. 3b shows the results of this validation, where $E^{\text{gb}}_{\text{AB}}$ is varied to produced different enthalpies of grain boundary segregation at different fixed values of E^{c}_{AB}, which controls the enthalpy of mixing (all other bond energies were fixed at 0 eV). Regardless of the enthalpy of mixing, the enthalpy of segregation calculated by Eq. 12 compared reasonably well with the enthalpy of segregation produced in the simulations.

The regular nanocrystalline solution (RNS) model also produces a similar equation for the enthalpy of grain boundary segregation [22]:

$$\Delta H_{\text{seg}} = \frac{z}{2}\left(2E^{\text{c}}_{\text{AB}} - E^{\text{c}}_{\text{AA}} + E^{\text{gb}}_{\text{AA}} - E^{\text{gb}}_{\text{AB}} - \frac{1}{2}(E^{\text{c}}_{\text{AA}} + E^{\text{c}}_{\text{BB}})\right) \tag{13}$$

When the enthalpy of mixing is zero, both Eqs. 12 and 13 are equivalent, but for non-zero enthalpies of mixing, the RNS model produces a systematic error because it assumes a random solution configuration and thus fails to account for the ordering preferred at the grain boundary. While the RNS equation is useful at the continuum level, when ordering at the grain boundary is present the approach outlined above produces a more reliable equation for grain boundary segregation enthalpy. For a given grain boundary compound, stability and metastability criteria can be derived from Eqs. 10 and 11 using the relationship in Eq. 12, $\Delta H_{\text{form}} = \frac{z}{2}\left[E^{\text{c}}_{\text{A}_\text{x}\text{B}} - (1 - x_s^c)E^{\text{c}}_{\text{AA}} - x_s^c E^{\text{c}}_{\text{BB}}\right]$, and $k\gamma = \frac{z}{2}[E^{\text{gb}}_{\text{AA}} - E^{\text{c}}_{\text{AA}}]$. The criteria for the stability and metastability of this grain boundary compound are thus:

$$\text{Stability: } E^{\text{gb}}_{\text{AB}} + E^{\text{c}}_{\text{AB}} - 2E^{\text{c}}_{\text{AA}} < \frac{1}{x_s^c}\left(E^{\text{c}}_{\text{A}_\text{x}\text{B}} - E^{\text{c}}_{\text{AA}}\right) \tag{14}$$

$$\text{Metastability: } E^{\text{gb}}_{\text{AB}} < E^{\text{c}}_{\text{AB}} \tag{15}$$

Under the assumption that the alloy has a positive enthalpy of mixing and that BB and AA bonds have the same energy this criterion is exactly the same as that established by Chookajorn and Schuh [41], but it is substantially more general in the present form, as it applies to any second phase and can be derived for any grain boundary compound in a lattice model.

5. Monte Carlo Simulations

The lattice model is solved through a Monte Carlo simulation in order to study more complicated behavior of both the grain boundary and the bulk states as a function of composition and temperature. Monte Carlo also doesn't require an assumption that grain boundary complexions

behave energetically like phases. Thus using Monte Carlo, we can similarly explore the generality of both the stability and metastability criteria established in the previous sections, this time including configurational entropy and geometric constraints, and unearth more nuanced behavior within the stable and metastable regimes for nanocrystalline alloys.

Monte Carlo simulations were conducted on a 72x72x8 BCC lattice. The lattice was initiated with a random distribution of solute and with a unique grain number assigned to each lattice site. Atom and grain swaps, as proposed by Chookajorn and Schuh [41], were used to explore the configuration space until $4x10^9$ Monte Carlo swaps were attempted, starting from a temperature of 10,000°C and reducing the temperature towards a final temperature of 500°C at a rate of 0.1% every Monte Carlo step (equivalent to $4x10^4$ swap attempts). Using the compound unit approach [47], a $D0_3$ compound (25 at.% stoichiometry) with an enthalpy of formation of -20 kJ/mol was incorporated into the configuration space of the model. Simulations were conducted varying the ΔH_{mix} and ΔH_{seg} as shown by the circles in the stability map in Fig. 2, with $k\gamma$ = 20 kJ/mol and for a solute concentration of 10 at.%. Two series of simulations are described on Fig. 2, and will be discussed in turn in what follows:

- ΔH_{seg} series: the effect of grain boundary segregation tendency on equilibrium nanostructure.
- ΔH_{mix} series: the effect of second-phase formation tendency on equilibrium nanostructure.

5.1. The ΔH_{seg} series

Fig. 4 shows the results of increasing ΔH_{seg} at a fixed $\Delta H_{\mathrm{mix}} =$ -40 kJ/mol. Eq. 10 expects that a nanocrystalline state will be stable against grain growth and compound formation when

$\Delta H_{\text{seg}} > 60$ kJ/mol. Below ΔH_{seg} = 60 kJ/mol, bulk single crystalline states with a stable $D0_3$ compound are found, as expected. However, at 50 kJ/mol, a nanocrystalline state is found, wherein both grain boundary segregated states exist and $D0_3$ precipitates form. This state resembles a duplex nanocrystalline state [42] where the nanocrystallinity is stabilized entropically; rather than the ordered precipitate disordering into a solid solution at higher temperatures, it can instead disorder into a grain boundary segregated state, which can occur at a lower enthalpic cost when ΔH_{seg} is close to meeting the stability criterion. Evidence of the entropic nature of this stabilization is seen in Fig. 5, where in the region between 40-60 kJ/mol, the enthalpy of the equilibrium state increases as there is still an enthalpic cost to forming grain boundaries in accordance with Eq. 10.

Above ΔH_{seg} = 60 kJ/mol, stable nanocrystalline states are formed without the presence of an ordered precipitate, because a grain boundary compound is preferred to bulk ordering as predicted by the stability criterion. The grain boundary regions in the alloy at ΔH_{seg} = 60 kJ/mol are thick, and this thickness is reduced as ΔH_{seg} is increased. Correspondingly, there is less solute dissolved in the crystalline regions, which suggests that at higher ΔH_{seg} the alloy prefers thinner complexions because it can attain more entropy without having to dissolve into the grains at a higher enthalpic cost.

Metastability can be simulated by setting the formation energy of the $D0_3$ compound to zero; the resulting equilibrium microstructures are also shown in Fig. 4. Above 20 kJ/mol, grain boundary states are seen in the equilibrated structure, which matches the metastability threshold provided by Eq. 11. Interestingly, rather than forming a grain boundary network, at low ΔH_{seg} a precipitated “grain boundary phase” clusters together. This is an expected behavior for a system in which it is energetically degenerate to add grain boundary area or thicken existing grain

boundaries, which is a characteristic of a rule-of-mixtures on enthalpy. Such a "grain boundary phase" has been discussed in the regular nanocrystalline solution (RNS) model, which also exhibits this degeneracy, and can be interpreted as, e.g., an amorphous phase [23, 24].

However, there remains the general trend of stabilizing thinner grain boundaries when an alloy possesses a higher ΔH_{seg}, and in a similar way the states with a "grain boundary phase" have a higher solute concentration in the grain. At higher ΔH_{seg}, the grain boundary segregated state becomes more favorable (and forming a solid solution becomes less favorable), and as a result the alloy seems to prefer forming a grain boundary network which has more configurational entropy than the "grain boundary phase". This transition occurs when ΔH_{seg} is roughly 60 kJ/mol, where there is a corresponding change in slope in Fig. 5. The slope of the "grain boundary phase" is larger, which suggests that a lower enthalpy could be effected by forming such a precipitate even at higher enthalpies of segregation, and thus the stability of a grain boundary network would only be expected if entropy is playing a significant role. The network has a much larger interfacial area with the surrounding crystalline regions than does the precipitate, thus the solute configurational entropy should be higher for the network configuration because solute at this interface will have a larger range of degenerate sites.

However, the grain topology space is explored in the present Monte Carlo simulations only through local changes to the grain numbers, which may not produce an ergodic sampling of grain boundary configuration space and prohibits detailed exploration of the preference for the network configuration. It is a future direction of our research to explore different Monte Carlo sampling mechanisms for exploring the grain boundary configuration space. We are not aware that the configurational entropy of grain boundary networks has been elaborated in detail, although for nanostructured systems this is clearly a necessary component of their thermodynamics and is

worthy of further study. Quantitative separation of entropy from such simulations is another direction of our future work.

5.2. The ΔH_{mix} series

The behavior when changing ΔH_{mix} is quite different than when changing only the enthalpy of grain boundary segregation (Fig. 6). When the $D0_3$ compound is present, there is a change from a duplex structure to a fully grain boundary segregated structure, which occurs in accordance with Eq. 10. However, while the stability is increased as the enthalpic benefit for bulk ordering is decreased, the equilibrium nanostructure is roughly unchanged. This is similarly observed when metastable equilibrium is studied, where grain sizes remain relatively large and unchanged with ΔH_{mix}. This suggests that it is the relative stability of the alloy with respect to the metastability criteria that governs behavior, which is reasonable since the stability criterion accounts for the possibility of compound formation, and if the compound is not formed, its existence in the phase space should not affect the equilibrium properties. Fig. 7 shows the effective grain boundary energy at different solute concentrations, calculated in the same manner as in Ref. [41], when two key quantities in the stability criteria are changed: $\Delta H_{\mathrm{mix}} - \frac{1}{x_{\mathrm{s}}^{\mathrm{c}}}\Delta H_{\mathrm{form}}$ and $\Delta H_{\mathrm{seg}} - k\gamma$. This quantitatively shows that changing $\Delta H_{\mathrm{mix}} - \frac{1}{x_{\mathrm{s}}^{\mathrm{c}}}\Delta H_{\mathrm{form}}$ does not affect the energy of the grain boundary segregated state, and only $\Delta H_{\mathrm{seg}} - k\gamma$ is relevant. Typically ΔH_{mix} is necessary for determining the critical temperature at which an ordered state will disorder, but in this case ΔH_{seg} already incorporates this effect (see Eq. 9) and as a result it is the key alloying parameter that governs the thermodynamic behavior of the nanocrystalline state.

6. Guidelines for Nanocrystalline Alloy Selection

A selection of binary alloys for which stabilization of the nanocrystalline state by grain boundary segregation has been studied experimentally [17, 19, 31, 33, 42, 51-53] are listed in Table 1 with the relevant bulk thermodynamic parameters for each alloy system (obtained as described in Section 2). The position of each system with respect to the present stability and metastability criteria is also indicated.

First examining the Fe-based alloys [17,31,52-54], Darling and coworkers found that alloying with 1 at.% Zr stabilized a grain size of 50 nm up to 1000°C without the formation of any precipitates [17]. However, when alloying with 10 at.% Zr, the precipitation of an Fe_2Zr phase was observed at 700°C leading to a loss of thermal stability [31]. Similar behavior was observed by Clark et al. when alloying Fe with 10 at.% Mg [52] and by Liu when alloying Fe with 3.2 at.% Ag [53], i.e. grain boundary segregation is observed to help retain nanometer-scale grain sizes and upon annealing second phase precipitation is found. The stability criterion predicts Fe-Zr and Fe-Mg to be borderline stable candidates and Fe-Ag to be metastable as the grain boundary segregated state does not present a substantial decrease in enthalpy compared to the alternative of forming second phases. This is reasonably consistent with the experimental observations considering the approximate nature with which thermodynamic parameters have been determined for these systems. It is important to also note that unlike in the Fe-Zr system the grain size in the Fe-Mg and Fe-Ag systems is not observed to become constant with increasing temperature. Thus, more data is needed to determine whether the Mg and Ag-alloyed systems are metastable or unstable, as their behavior is also similar to Fe-Cu [52,54], Fe-Ta [17], Hf-Ti [55], and Ni-W [33] nanocrystalline alloys which have a much lower enthalpy of grain boundary segregation. For example, Fe with 1

at.% Ta underwent rapid, abnormal grain growth at 800°C without the precipitation of a second phase, which may be evidence that the nanostructure stability at lower homologous temperatures is in part due to solute drag. Alternatively, the temperature dependence of segregation may come into play in systems such as this, where dissolution into the bulk is favored upon heating; entropic desegregation of the boundaries would certainly lead to a loss of stability, although we are not aware of any detailed study on that topic to date.

In W-based alloys, the addition of 20 at.% Ti was found to stabilize a 20 nm grain size after annealing at 1100°C for 1 week [16] through grain boundary segregation with no second phase precipitation. In contrast, annealing tungsten with 15 at.% Cr at 950°C [42] also provides stability through grain boundary segregation but also leads to second phase formation and is thus metastable. While the enthalpy of grain boundary segregation is similar in both alloys, the enthalpy of mixing is almost twice as high for W-Cr, which explains the difference in behavior of these systems in accordance with Eqs. 10 and 11.

Many alloying systems studied for stabilizing nanocrystalline materials through grain boundary segregation are positive enthalpy of mixing couples. This is in part due to a general, albeit weak, correlation expected between enthalpy of mixing and enthalpy of grain boundary segregation, but also a consequence of many stability models being limited to only considering positive enthalpy of mixing alloys. The criteria presented here, with the incorporation of negative enthalpy of mixing systems and consideration of ordered phases, should enable a more systematic and unconstrained exploration of alloy systems.

7. Conclusions

A framework for selecting alloying elements that can stabilize a nanocrystalline structure is developed. The key results are:

- A stability criterion for a nanocrystalline state in terms of macroscopic thermodynamic properties is developed: $\Delta H_{\text{seg}} > \Delta H_{\text{mix}} - \frac{1}{x_s^c}\Delta H_{\text{form}} + k\gamma$ by comparing the enthalpy of a grain boundary segregated state and competing bulk phases (Section 2).
- A framework for translating known macroscopic thermodynamic properties into a lattice model is developed to enable consideration of entropic and geometric effects (Section 4). Lattice-based Monte Carlo simulations largely verify the stability criteria that was developed analytically (Figs. 4-7).
- The simulations show that entropy can contribute to stabilization of the grain boundary segregated state and enable the formation of a duplex structure with the precipitation of an ordered compound in a nanocrystalline state.
- The simulations also suggest that entropy can play a role in the preference to form a network of grain boundaries instead of an amorphous cluster.

8. Acknowledgements

This work was supported by the U.S. Army Research Office under grant W911NF-14-1-0539. ARK would like to acknowledge the support of a National Defense Science and Engineering Graduate Research Fellowship.

References

1. K. A. Darling, M. Rajagopalan, M. Komarasamy, M. A. Bhatia, B. C. Hornbuckle, R.S. Mishra, K. N. Solanki, Extreme creep resistance in a microstructurally stable nanocrystalline alloy. Nature 537 (2016) 378-381.

2. G. Liu, G J. Zhang, F. Jiang, X. D. Ding, Y. J. Sun, J. Sun, Nanostructured high-strength molybdenum alloys with unprecedented tensile ductility, Nat. Mater. 12 (2013) 344-350.

3. P.V. Liddicoat, X.Z. Liao, Y. Zhao, Y. Zhu, M. Y. Murashkin, E. J. Lavernia, R. Z. Valiev, S. P. Ringer, Nanostructural hierarchy increases the strength of aluminium alloys, Nat. Comm. 1 (2010) 1-7.

4. M. A. Meyers, A. Mishra, D. J. Benson, Mechanical properties of nanocrystalline materials, Prog. Mater. Sci. 51 (2006) 427-556.

5. P. G. Sanders, J. A. Eastman, J. R. Weertman, Elastic and tensile behavior of nanocrystalline copper and palladium, Acta Mater. 45 (1997) 4019-4025.

6. M. S. Dresselhaus, G. Chen, M. Y. Tang, R. G. Yang, H. Lee, D. Z. Wang, Z. F. Ren, J. P. Fleurial, P. Gogna, New directions for low-dimensional thermoelectric materials, Adv. Mater. 19 (2007) 1043-1053.

7. G. Herzer, Grain size dependence of coercivity and permeability in nanocrystalline ferromagnets, IEEE Trans. Magn. 26 (1990) 1397-1402.

8. A. Manaf, R. A. Buckley, H. A. Davies, New nanocrystalline high-remanence Nd-Fe-B alloys by rapid solidification, J. Magn. Magn. Mater. 128 (1993) 302-306.

9. H. Natter, M. Schmelzer, R. Hempelmann, Nanocrystalline nickel and nickel-copper alloys: Synthesis, characterization, and thermal stability, J. Mater. Res. 13 (1998) 1186-1197.

10. C. H. Moelle, H. J. Fecht, Thermal stability of nanocrystalline iron prepared by mechanical attrition, Nanostruct. Mater. 6 (1995) 421-424.

11. M. Thuvander, M. Abraham, A. Cerezo, G. D. Smith, Thermal stability of electrodeposited nanocrystalline nickel and iron–nickel alloys, 17 (2001) 961-970.

12. H. Natter, M. Schmelzer, M. S. Löffler, C. E. Krill, A. Fitch, R. Hempelmann, Grain-growth kinetics of nanocrystalline iron studied in situ by synchrotron real-time X-ray diffraction, J. Phys. Chem. B, 104 (2000) 2467-2476.

13. J. Weissmüller, Alloy effects in nanostructures, Nanostruc. Mater. 3 (1993) 261-272.

14. P. Wynblatt, D. Chatain, Anisotropy of segregation at grain boundaries and surfaces, Metall. Mater. Trans. A 37 (2006) 2595-2620.

15. R. Kircheim, Reducing grain boundary, dislocation line and vacancy formation energies by solute segregation. I. Theoretical background, Acta Mater. 55 (2007) 5129-5138.

16. T. Chookajorn, H. A. Murdoch, C. A. Schuh Design of stable nanocrystalline alloys, Science, 337 (2012) 951-954.

17. K. A. Darling, B. K. VaLeeuwen, J. E. Semones, C. C. Koch, R. O. Scattergood, L. J. Kecskes, S. N. Mataudhu, Stabilized nanocrystalline iron-based alloys: Guiding efforts in alloy selection, Mater. Sci. Eng. A 528 (2011) 4365-4371.

18. P. Choi, M. da Silva, U. Klement, T. Al-Kassab, R. Kircheim, Thermal stability of electrodeposited nanocrystalline Co-1.1 at.% P, Acta Mater. 53 (2005) 4473-4481.

19. T. Chookajorn, C. A. Schuh, Nanoscale segregation behavior and high-temperature stability of nanocrystalline W–20at.% Ti, Acta Mater. 73, (2014) 128-138.

20. M. Park, C. A. Schuh, Accelerated sintering in phase-separating nanostructured alloys, Nat. Comm. 6 (2015) 1-6.

21. A. J. Detor, C. A. Schuh, Tailoring and patterning the grain size of nanocrystalline alloys, Acta Mater. 55 (2007) 371-379.

22. J. R. Trelewicz, C. A. Schuh, Grain boundary segregation and thermodynamically stable binary nanocrystalline alloys, Phys. Rev. B 79 (2009) 094112.

23. H. A. Murdoch, C. A. Schuh, Stability of binary nanocrystalline alloys against grain growth and phase separation, Acta Mater. 61 (2013) 2121-2132.

24. N. Zhou, J. Luo, Developing thermodynamic stability diagrams for equilibrium-grain-size binary alloys, Mater. Lett. 115 (2014) 268-271.

25. M. Saber, H. Kotan, C. C. Koch, R. O Scattergood, A predictive model for thermodynamic stability of grain size in nanocrystalline ternary alloys, J. Appl. Phys. 114 (2013) 103510.

26. A. R. Kalidindi, T. Chookajorn, C. A. Schuh, Nanocrystalline materials at equilibrium: A thermodynamic review, JOM 67 (2015) 2834-2843.

27. M. Saber, C. C. Koch, R. O. Scattergood, Thermodynamic grain size stabilization models: an overview, Mater. Res. Lett. 3 (2015) 65-75.

28. S. C. Mehta, D. A. Smith, U. Erb, Study of grain growth in electrodeposited nanocrystalline nickel-1.2 wt.% phosphorus alloy, Mater. Sci. and Eng. A 204 (1995) 227-232.

29. T. H. Hentschel, D. Isheim, R. Kircheim, F. Müller, H. Kreye, Nanocrystalline Ni–3.6 at.% P and its transformation sequence studied by atom-probe field-ion microscopy, Acta Mater. 48 (2000) 933-941.

30. P. Choi, M. da Silva, U. Klement, T. Al-Kassab, R. Kircheim, Thermal stability of electrodeposited nanocrystalline Co-1.1 at.% P, Acta Mater. 53 (2005) 4473-4481.

31. K. A. Darling, B. K. VanLeeuwen, C. C. Koch, R. O. Scattergood, Thermal stability of nanocrystalline Fe–Zr alloys, Mater. Sci. Eng. A 527 (2010) 3572-3580.

32. P. Choi, T. Al-Kassab, F. Gärtner, H. Kreye, R. Kircheim, Thermal stability of nanocrystalline nickel–18 at.% tungsten alloy investigated with the tomographic atom probe, Mater. Sci. Eng. A, 353 (2003) 74-79.

33. A. J. Detor, C. A. Schuh, Microstructural evolution during the heat treatment of nanocrystalline alloys, J. Mater. Res. 22 (2007) 3233-3248.

34. S. J. Dillon, M. Tang, W. C. Carter, M. P. Harmer, Complexion: A new concept for kinetic engineering in materials science, Acta Mater. 55 (2007) 6208-6218.

35. M. Guttman, Grain boundary segregation, two dimensional compound formation, and precipitation, Metall. Trans. A 8 (1977) 1383-1401.

36. R. Kirchheim, Physics and chemistry of segregation at internal interfaces, in: D. Wolf, S. Yip (Eds.), Materials interfaces, atomic-level structure and properties, Chapman & Hall, London, 1992, pp. 481-496.

37. J. F. Nie, Y. M. Zhu, J. Z. Liu, X. Y. Fang, Periodic segregation of solute atoms in fully coherent twin boundaries, Science 340 (2013) 957-960.

38. D. Raabe, M. Herbig, S. Sandlöbes, Y. Li, D. Tytko, M. Kuzmina, D. Ponge, P. P. Choi, Grain boundary segregation engineering in metallic alloys: A pathway to the design of interfaces, Curr. Opin. Solid State Mater. Sci. 19 (2014) 243-261.

39. T. Frolov, M. Asta, Y. Mishin, Segregation-induced phase transformations in grain boundaries, Phys. Rev. B 92 (2015) 020103.

40. A. Khalajhedayati, T. J. Rupert, High-temperature stability and grain boundary complexion formation in a nanocrystalline Cu-Zr alloy, JOM 67 (2015) 2788-2801.

41. T. Chookajorn, C. A. Schuh, Thermodynamics of stable nanocrystalline alloys: A Monte Carlo analysis, Phys. Rev. B 89 (2014) 064102.

42. T. Chookajorn, M. Park, C. A. Schuh, Duplex nanocrystalline alloys: Entropic nanostructure stabilization and a case study on W–Cr, J. Mater. Res. 30 (2015) 151-163.

43. J. E. Saal, S. Kirklin, M. Aykol, B. Meredig, C. Wolverton, Materials design and discovery with high-throughput density functional theory: the open quantum materials database (OQMD), JOM 65 (2013) 1501-1509.

44. S. Curtarolo, W. Setyawan, S. Wang, J. Xue, K. Yang, R. H. Taylor, L. J. Nelson, G. L Hart, S. Sanvito, M. Buongiorno-Nardelli, N. Mingo, O. Levy, AFLOWLIB. ORG: A distributed materials properties repository from high-throughput ab initio calculations, Comp. Mater. Sci. 58 (2012) 227-235.

45. A. Jain, S. P. Ong, G. Hautier, W. Chen, W. D. Richards, S. Dacek, S. Choila, D. Gunter, D. Skinner, G. Ceder, K. A. Persson, Commentary: The Materials Project: A materials genome approach to accelerating materials innovation, Appl. Mater. 1 (2013) 011002.

46. W. Xing, A. R. Kalidindi, C. A. Schuh, Preferred nanocrystalline configurations in ternary and multicomponent alloys, Scr. Mater. 127 (2017) 136-140.

47. A. R. Kalidindi, C. A. Schuh, A compound unit method for incorporating ordered compounds into lattice models of alloys, Comp. Mater. Sci. 118 (2016) 172-179.

48. H. A. Murdoch, C. A. Schuh, Estimation of grain boundary segregation enthalpy and its role in stable nanocrystalline alloy design, J. Mater. Res. 28 (2013) 2154-2163.

49. F. R. De Boer, W. C. Mattens, R. Boom, A. R. Miedema, A. K. Niessen, Cohesion in metals: Transition metal alloys, North-Holland, Amsterdam, 1988.

50. C. Kittel, Introduction to Solid State Physics, fourth ed., Malden, Massachusetts, 2005.

51. E. D. Hondros, M. P. Seah, Grain boundary activity measurements by Auger electron spectroscopy, Scr. Metall. 6 (1972) 1007-1012.

52. B. G. Clark, K. Hattar, M. T. Marshall, T. Chookajorn, B. L. Boyce, C. A. Schuh, Thermal stability comparison of nanocrystalline Fe-based binary alloy pairs. JOM 68 (2016) 1625-1633.

53. F. Liu, Grain growth in nanocrystalline Fe-Ag thin film. Mater. Lett. 59 (2005) 1458-1462.

54. J. Eckert, J. C. Holzer, W. L. Johnson, Thermal stability and grain growth behavior of mechanically alloyed nanocrystalline Fe-Cu alloys. J. Appl. Phys. 73 (1993) 131-141.

55. M. N. Polyakov, T. Chookajorn, M. Mecklenburg, C. A. Schuh, A. M. Hodge, Sputtered Hf-Ti nanostructures: A segregation and high temperature stability study. Acta Mater. 108 (2016) 8-16.

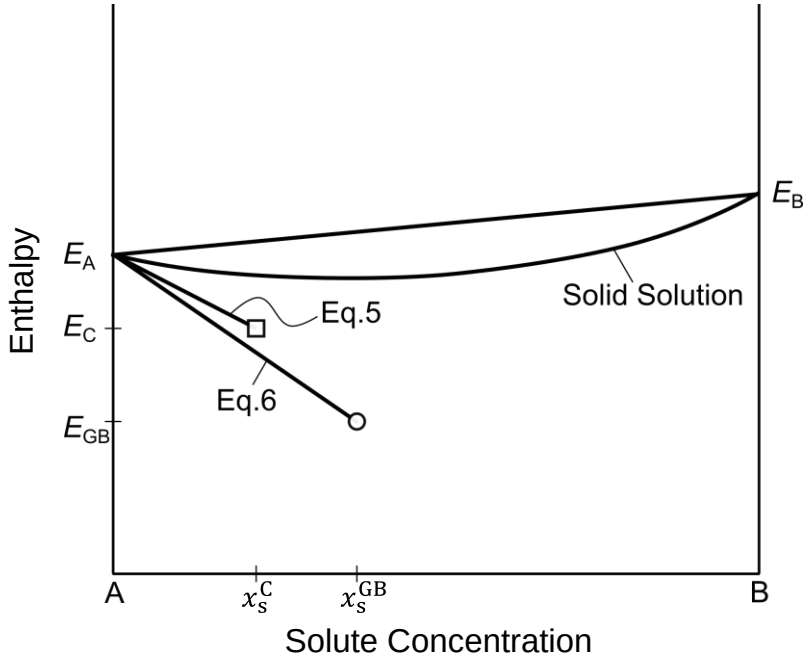

Figure 1. Schematic of the binary alloy energy diagram including an ordered phase (square) and a 2D grain boundary compound (circle) where the energy of non-stoichiometric compositions is calculated by the lever rule (lines).

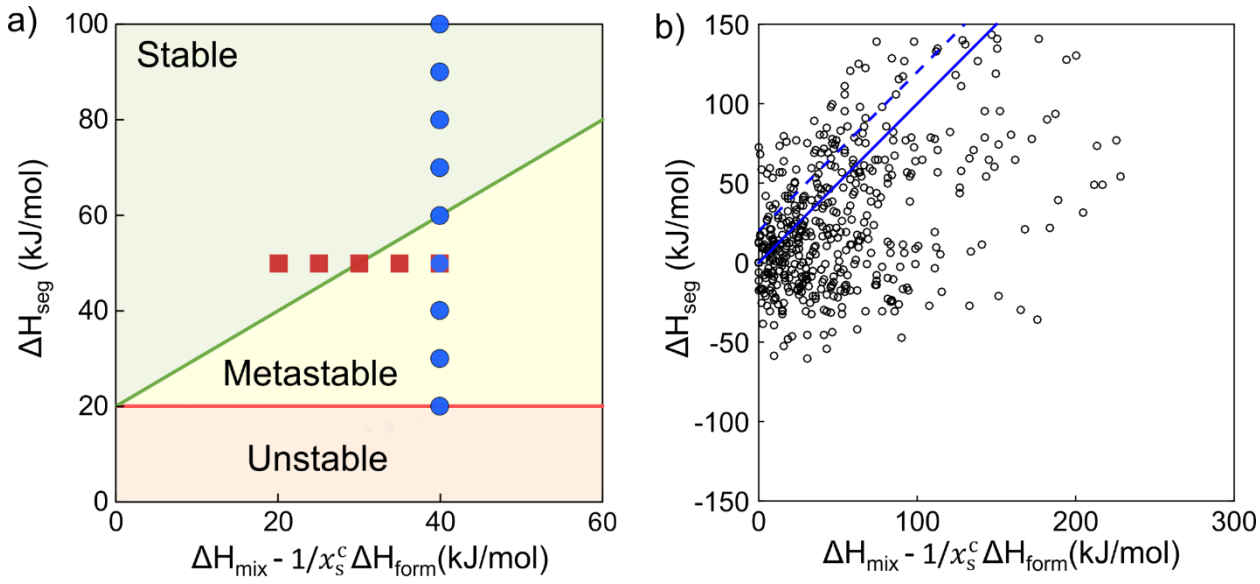

Figure 2. a) Stability map based on Eqs. 10 and 11, when $k\gamma$ = 20 kJ/mol. Blue dots correspond to the ΔH_{seg} series and the red squares correspond to the ΔH_{mix} series for which equilibrium nanostructures are shown in Figs. 4 and 6, respectively. b) Transition metal – transition metal binary alloys plotted using Miedema estimates [48, 49] of ΔH_{mix} and ΔH_{seg} and density functional theory calculations of ΔH_{form} for compounds (attained from the Open Quantum Materials Database [43]) to observe the strength of correlation between the two axes of the stability map for physical alloy pairs. The solid line corresponds to perfect correlation between the axes, and the dashed line represents the stability criterion.

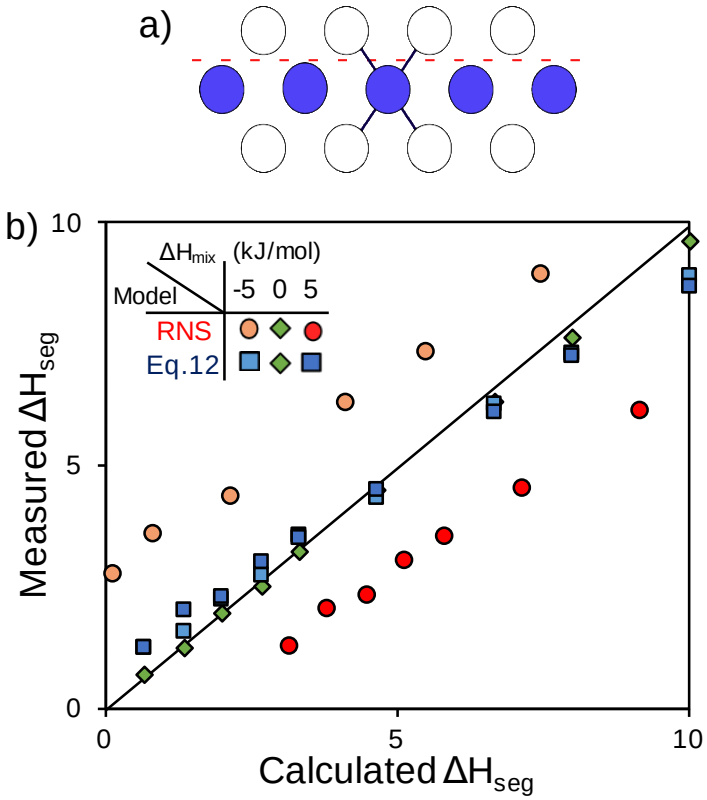

Figure 3. a) Schematic of ordering at a fixed grain boundary in the lattice model for a BCC lattice (blue – solute). b) Verification of Eq. 12 for calculating pairwise bond energies for the lattice model from a known enthalpy of segregation and a known grain boundary compound.

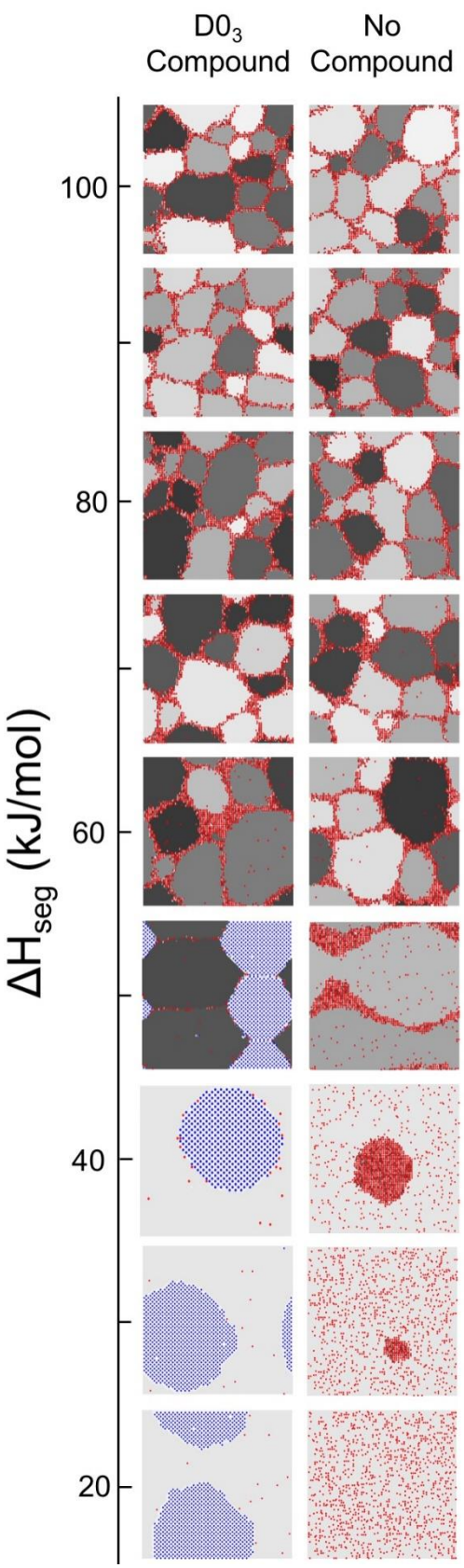

Figure 4. Equilibrium states of the ΔH_{seg} series with a stable $D0_3$ compound (on left) and systems without any stable compound (on right). Different grains have different shades of gray. Solute atoms are in blue if they are part of a $D0_3$ precipitate and red otherwise.

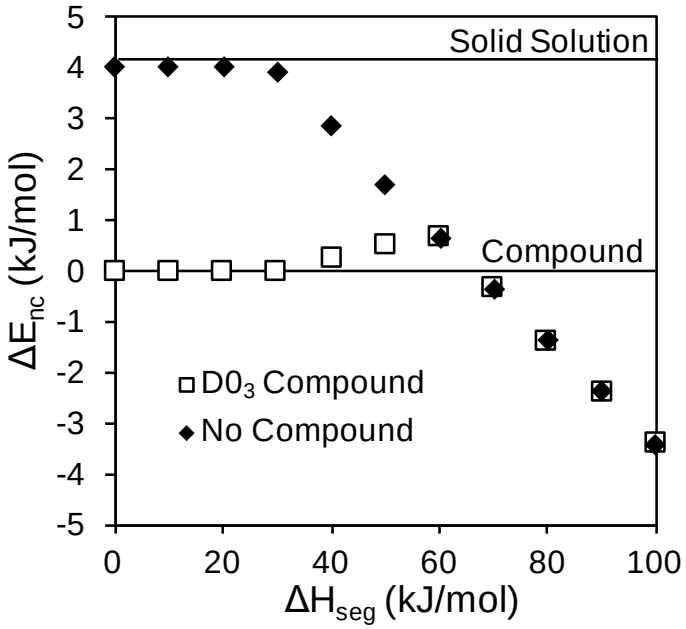

Figure 5. The enthalpy relative to the bulk equilibrium state with increasing enthalpy of segregation for alloy systems with a stable $D0_3$ compound and without any stable compound.

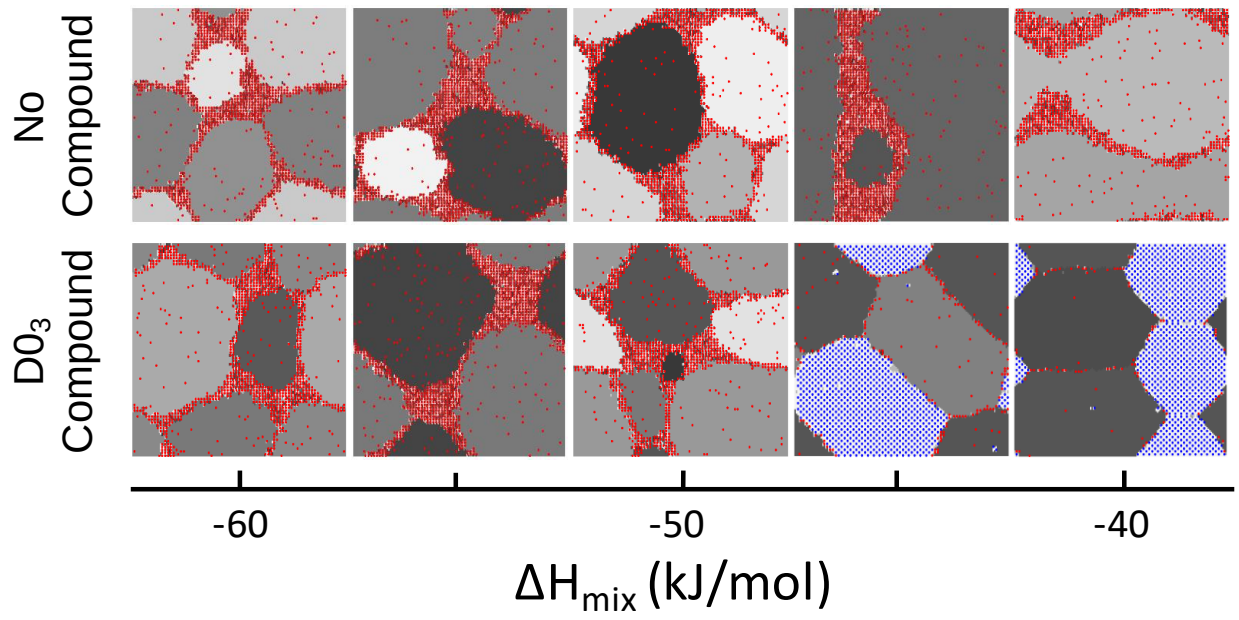

Figure 6. Equilibrium states of the ΔH_{mix} series with a stable $D0_3$ compound (bottom) and without any stable compound (top). Different grains have different shades of gray. Solute atoms are in blue if they are part of a $D0_3$ precipitate and red otherwise.

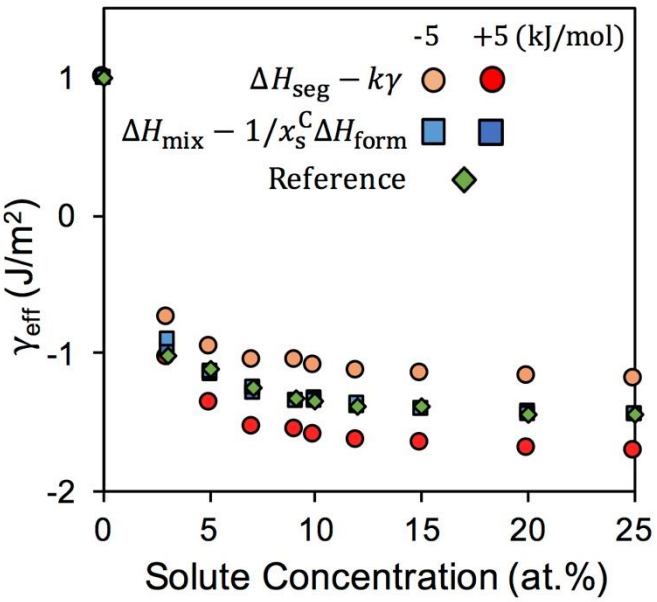

Figure 7. Effect on the excess enthalpy of the grain boundary segregated state, upon varying the enthalpy of grain boundary segregation and the enthalpy of mixing independently.

Table 1. Predicted stability classification according to Eqs. 10 and 11 for alloy systems for which the thermal stability has been experimentally studied. ΔH_{seg} critical is the enthalpy of grain boundary segregation needed for the alloy system to be stable. If the enthalpy of grain boundary segregation is within 5 kJ/mol of satisfying or failing either criteria, both likely classifications are specified.

Alloy	ΔH_{seg} (kJ/mol)	ΔH_{mix} (kJ/mol)	x_S^C	ΔH_{form} (kJ/mol)	kγ (kJ/mol)	ΔH_{seg} critical (kJ/mol)	Stability
Fe-Zr	61	-35	1/3	-27	12	58	Stable/Metastable
Fe-Mg	86	76	1	0	12	84	Stable/Metastable
Fe-Ag	58	128	1	0	12	140	Metastable
Fe-Cu	19	52	1	0	12	64	Metastable
Fe-Ta	15	-10	1/3	-19	12	59	Metastable/Unstable
W-Ti	65	20	1	0	24	44	Stable
W-Cr	61	38	1	0	24	62	Metastable/Stable
Ni-W	10	-3	1/5	-10	10	57	Metastable/Unstable
Hf-Ti	28	14	1	0	19	33	Metastable